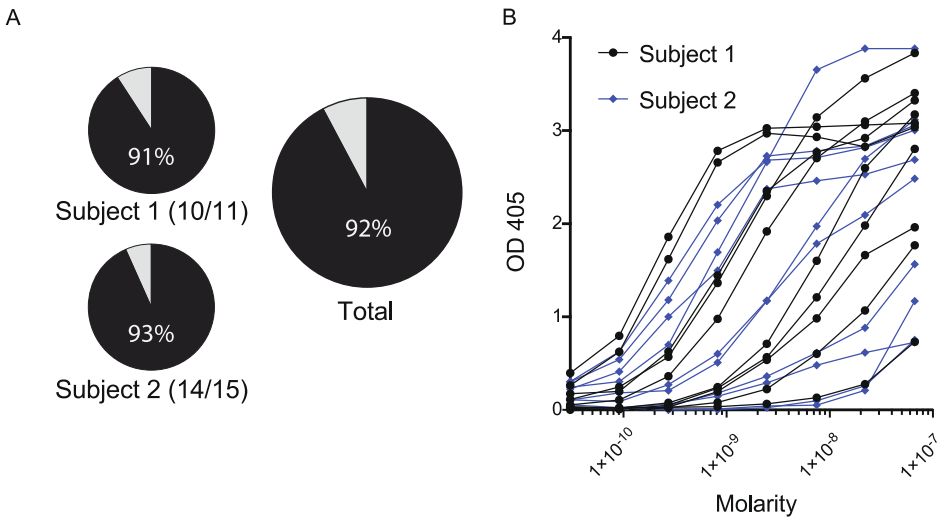

Fig. S1. Validation of the HA binding FACS assay. Monoclonal antibodies were generated from single cell sorted CD19+CD27+ HA binding B cells isolated from two individuals that received the seasonal influenza vaccine. ELISAs were performed to test the specificity of the monoclonal antibodies to HA. (**A**) Percentage of monoclonal antibodies derived from HA+ memory B cells that bind vaccine by ELISA in each subject. (**B**) ELISAs binding curves of antibodies from (**A**).

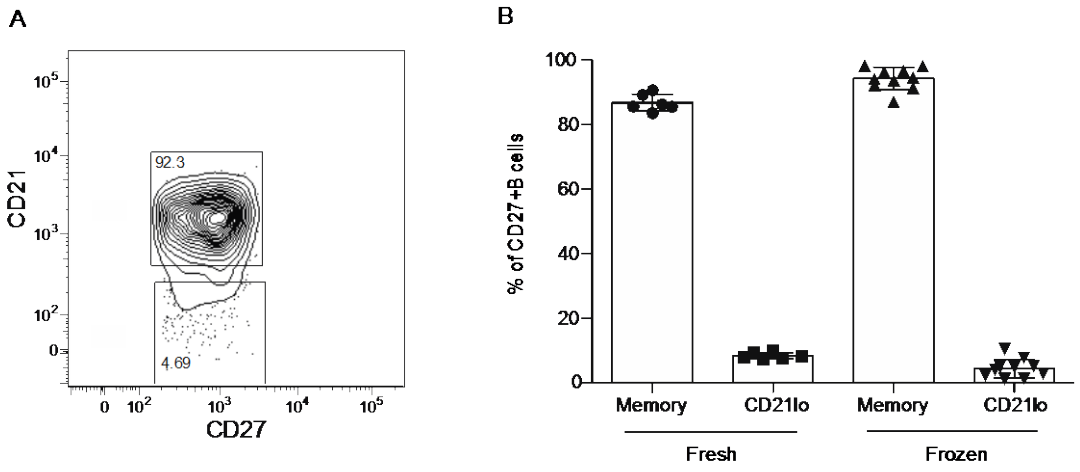

Fig. S2. CD21lo cells can be isolated from frozen PBMC. Whole PBMCs were isolated from peripheral blood using a Ficoll gradient 14 days post immunization with the 2013-2014 or 2014-2015 seasonal influenza vaccine. PBMCs were stored in liquid nitrogen in FCS with 10% DMSO until they were thawed and analyzed. (**A**) Representative gating of memory and CD21lo cells in the CD27+ B cell compartment from thawed PBMCs. (**B**) Percentage of memory and CD21lo cells in the CD27+ B cell compartment in freshly isolated blood (n=6) or after freeze thaw (n=10). Bar graphs represent the mean (+/- SD).

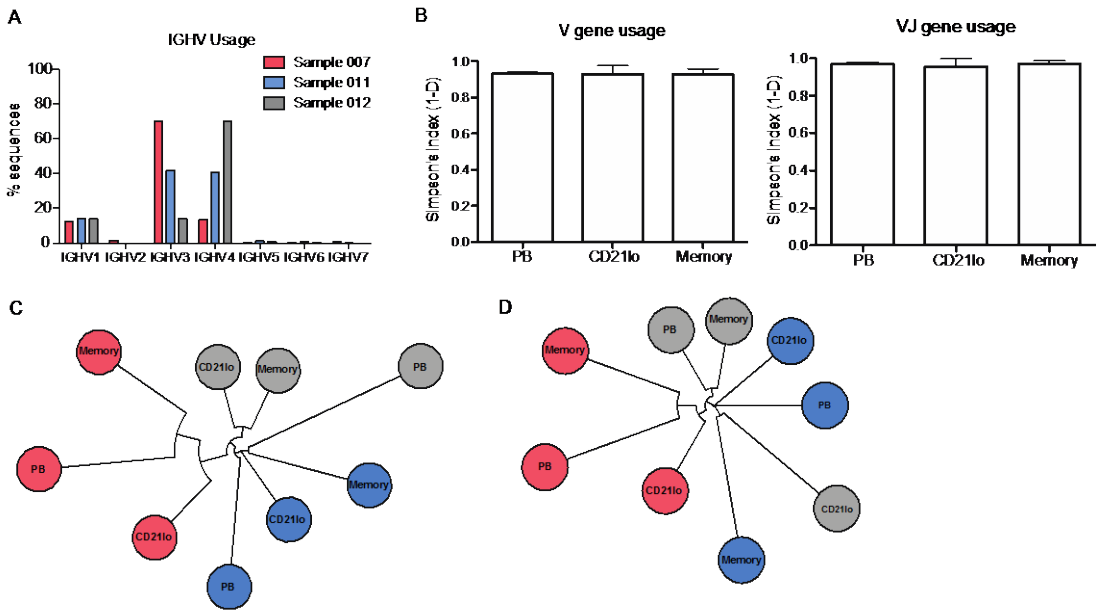

Fig. S3. PB, CD21lo and memory cells are diverse in their immunoglobulin gene usage. Variable gene usage was analyzed from high throughput immunoglobulin gene sequencing. Variable gene alignment was performed with IMGT High VQUEST. (**A**) Frequency of usage of genes from each IGHV family. (**B**) Diversity in IGHV gene usage and IGHV-IGHJ gene pairings as measured by Simpson's Index. Index represents the probability that two randomly drawn sequences will not be the same gene (or gene pair). Bars show mean diversity index (+/-SD). (**C**) Neighbor joining trees built from frequency vectors of IGHV gene usage or (**D**) IGHV-IGHJ gene pairings.

Fig. S4. Phylogenetic trees of experimentally validated flu binding clones. Repertoire sequencing data was filtered to identify clones that contained the same CDR3 sequence as experimentally confirmed flu binding antibodies. (**A**) Maximum likelihood trees were generated using RAxML[60] to determine the phylogenetic relationships between the different B cell subsets.

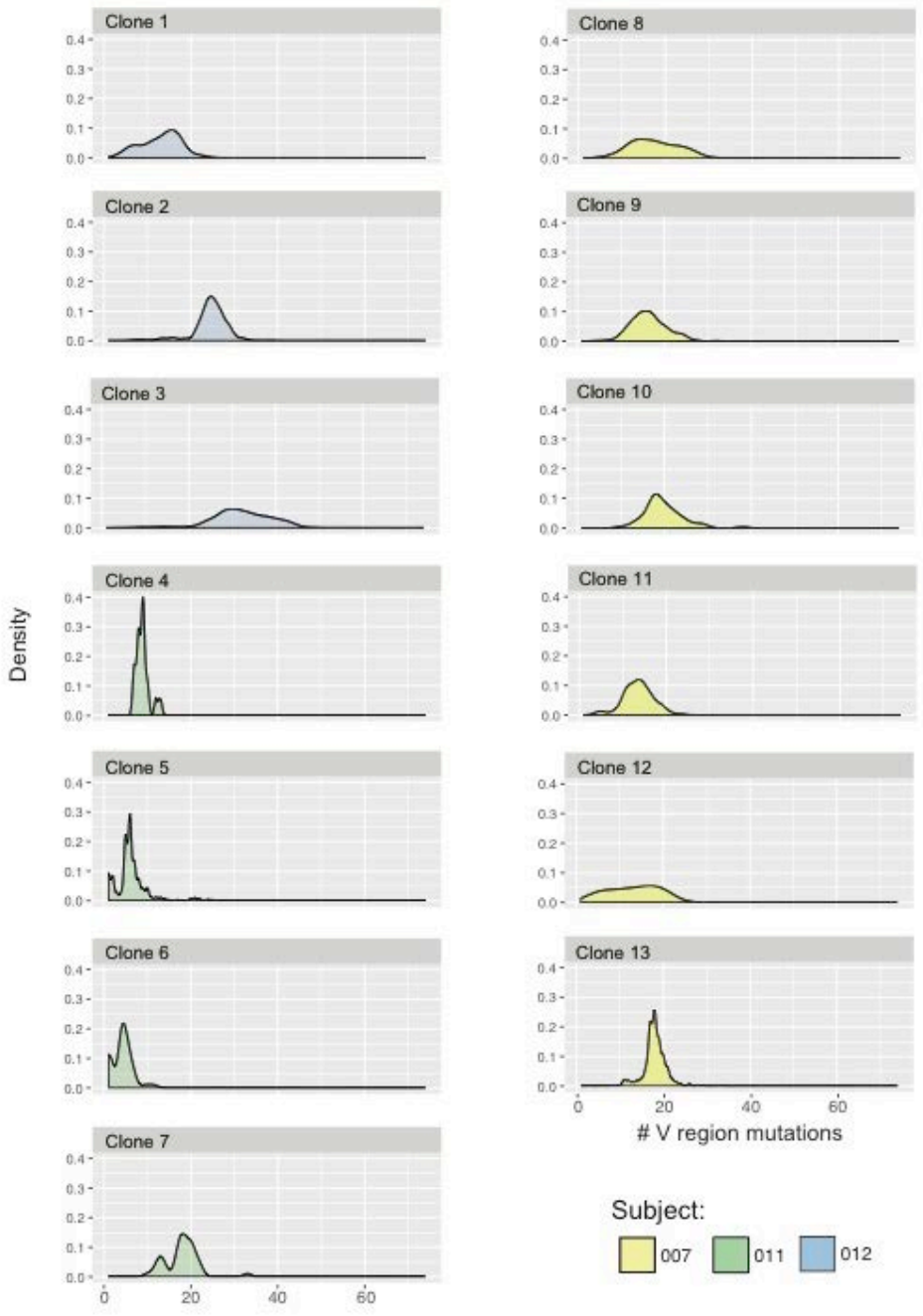

Fig. S5. Mutational load in influenza-reactive clones. The number of mutations of each sequence in the influenza-reactive clones was determined using IMGT High VQUEST. (**A**) Distribution of number of V region nucleotide mutations within clones containing experimentally validated influenza binding antibodies

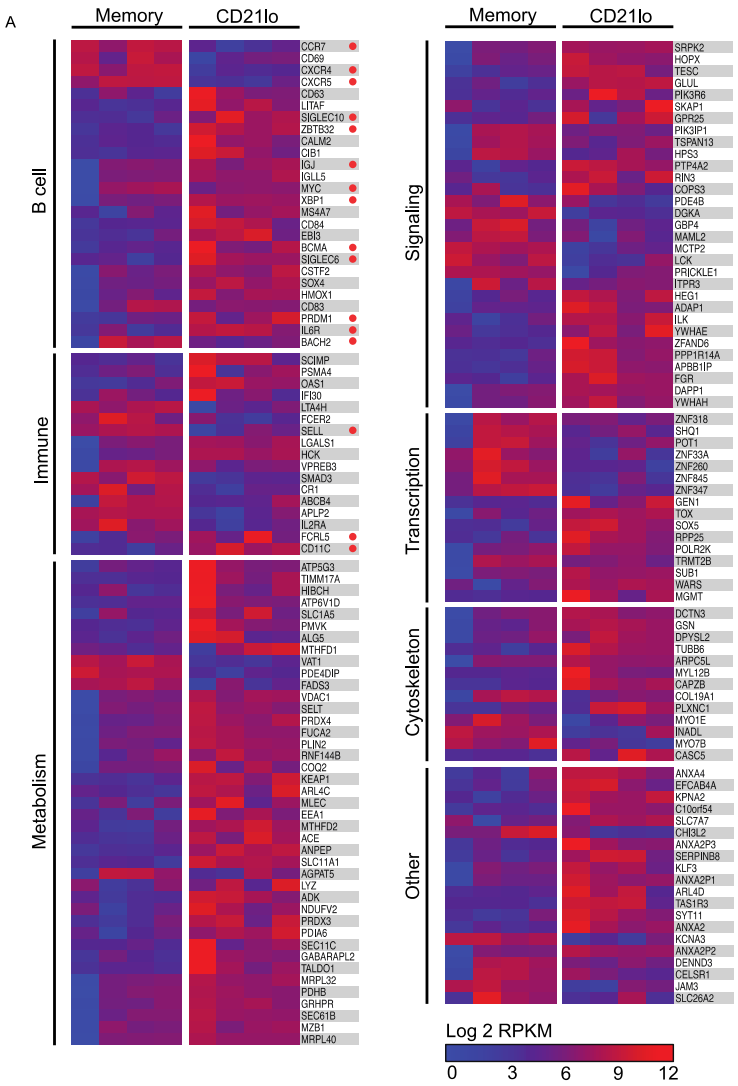

Fig. S6. Differential gene expression between CD21lo and memory B cells. RNASeq was performed on CD21lo and memory B cells isolated 14 days post-immunization. Sequence alignment and differential gene expression was analyzed using the Tuxedo suite on Galaxy. (**A**) Heatmap representing the expression (log2 RPKM) of selected differentially expressed genes (FDR < 0.05). Red dots represent genes highlighted in the text.

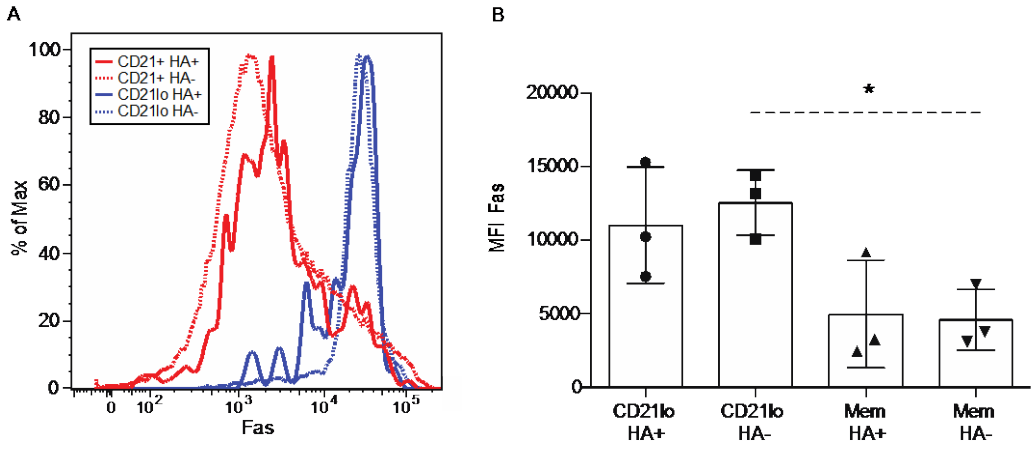

Fig. S7. CD21o cells have elevated protein levels of Fas, independent of HA specificity. Flow cytometry analysis was performed on fresh PBMCs isolated 21 days after immunization with the 2016-2017 seasonal influenza vaccine. (**A**) Representative histograms from FACS analysis of Fas expression on HA+ and HA- CD21lo and memory B cells. (**B**) Fas surface expression as represented by the MFI (median fluorescence intensity) (n=3). Statistical significance is calculated using a paired student t-test (*, $p < 0.05$). Bar graphs represent mean (+/- SD).

Sample	Ab name	H1N1	H3N2	B	CDR3
007-10051	2C06			●	gcgagaatgttttcctcgtacttttttgacttc
007-10051	2D02			●	gcgagaatgttttcttcgtactattttgactac
011-10069	2A01	●	●	●	gcgagaggcggaaatgggcgacccttttgacaac
011-10069	2F01	●	●		gcccgcgggggtgactcgggcggtgggctcgactac
011-10069	3B01	●	●	●	gcgagggcctattttgactcc
011-10069	3B03	●	●		gcgagaaggtactttgactac
011-10069	3D03		●		gcgcgagatgggagtgatactacgctgcctgtatattattatgatagtagtggccttgactac
012-10081	4D03		●		gcgagagatctgtatagcaccagttggtatgagcccagatttaactactactacggtatggacgtc
012-10081	4G05	●			gcgagagggctcggcattcttaacgttgacacacctatcatggactactttgactac

Table S1. Specificity of influenza-reactive antibodies. Monoclonal antibodies from all three subjects were generated from plasmablasts isolated 7 days post-vaccination. The specificity for each antibody was tested using ELISAs against influenza virus. The table shows the strain specificity and CDR3 sequences of monoclonal antibodies used to identify influenza-reactive clones in the immunoglobulin repertoire sequencing.